Superradiance-Mediated Photon Storage for Broadband Quantum Memory

Anindya Rastogi,[1,*] Erhan Saglamyurek,[1,2] Taras Hrushevskyi,[1] and Lindsay J. LeBlanc[1,†]
[1]Department of Physics, University of Alberta, Edmonton, Alberta T6G 2E1, Canada
[2]Department of Physics and Astronomy, University of Calgary, Calgary, Alberta T2N 1N4, Canada

(Received 19 December 2021; revised 30 July 2022; accepted 30 August 2022; published 13 September 2022)

Superradiance, characterized by the collective, coherent emission of light from an excited ensemble of emitters, generates photonic signals on timescales faster than the natural lifetime of an individual atom. The rapid exchange of coherence between atomic emitters and photonic fields in the superradiant regime enables a fast, broadband quantum memory. We demonstrate this superradiance memory mechanism in an ensemble of cold rubidium atoms and verify that this protocol is suitable for pulses on timescales shorter than the atoms' natural lifetime. Our simulations show that the superradiance memory protocol yields the highest bandwidth storage among protocols in the same system. These high-bandwidth quantum memories provide unique opportunities for fast processing of optical and microwave photonic signals, with applications in large-scale quantum communication and quantum computing technologies.

DOI: 10.1103/PhysRevLett.129.120502

Photonic emission from a collection of identical excited atoms under superradiant conditions is very different from that of a single-atom in free-space [1]. Comprehensive studies of superradiance [2–4] have led to the observation of various quantum optics phenomena like quantum beats [5], collective Lamb shifts [6,7], and novel cavity QED [8]. Initial studies focused on dense ensembles with sizes smaller than the excitation wavelength, whereas recent ones show that superradiance is also observable in large and dilute systems [9,10]. Large atomic ensembles, providing a high degree of experimental control, are especially amenable to superradiant effects: when an ensemble with moderate optical density ($d > 1$) is coherently excited by a temporally short (broadband) and weak probe, a subsequent radiation burst is emitted along the forward direction of the incident pulse [11–15]. The characteristic decay time of this emission is inversely proportional to the medium's optical depth and, for $d \gg 1$, can be much shorter than the spontaneous-emission lifetime of a single atom [5,9,10,16–20]. This optical-depth dependence of decay time is the hallmark of superradiant emission, different from the free-induction-decay (FID) of atomic dipoles among inhomogeneously broadened emitters [21,22].

Optical quantum memories [23–25] can take advantage of this rapid superradiant emission for broadband operation [21,26,27]. Here, we demonstrate a spin-wave memory based on superradiance [4,28] in a cloud of laser-cooled ^{87}Rb atoms featuring a homogeneously broadened optical transition. The superradiance (SR) mediated memory requires an initial excitation of the polarization coherence, followed by a second (fast) storage step, realizing a distinct memory mechanism that is inherently broadband and, in our experiments, is demonstrated without contribution from physical processes associated with other memory protocols. We find that the SR memory offers the most relaxed optical depth requirement for broadband signals in systems where the absorption linewidths are much narrower than the signal bandwidth to be stored. The inherently fast storage capability of this memory paves the way for bandwidth compatibility with conventional single-photon sources and high-speed quantum networks [29,30].

To understand the SR memory, consider an N-atom ensemble whose energy levels form a Λ configuration, where two ground-state spin levels $|g\rangle$ and $|s\rangle$ are optically coupled to an excited level $|e\rangle$. We assume that all atoms initially populate $|g\rangle$, and that both $|e\rangle \leftrightarrow \{|g\rangle, |s\rangle\}$ transitions are homogeneously broadened, with Lorentzian line shapes of characteristic width Γ and optical decoherence rates $\gamma = \Gamma/2$. A weak probe field (the optical signal to be stored) is resonant with the $|g\rangle \leftrightarrow |e\rangle$ transition, and a strong control field (to initiate probe storage or recall) with Rabi frequency $\Omega_C(t)$ drives the $|e\rangle \leftrightarrow |s\rangle$ transition. Resonant interactions between the optical fields and ensemble are described by the coupled Maxwell-Bloch equations in terms of coherences in the photonic ($\hat{E}$), polarization ($\hat{P}$), and spin-wave ($\hat{S}$) modes [27,31–34]. For the input probe, we consider an exponentially rising temporal profile of the form $I_P(t) = I_0 e^{(t-\tau)/T_P} u(\tau - t)$ (τ is the abrupt switch-off time); characteristic duration $T_P \ll 1/\gamma$ (Fig. 1); and bandwidth $B = 0.157/T_P$ [34], such that memory operation is broadband with $2\pi B \gg \Gamma$.

The SR memory protocol (Fig. 1) proceeds via three stages: absorption, writing, and retrieval, which follow the general principles of "fast Λ-type" storage and readout [27,31], and can also be extended to the "ladder-type" atomic configurations [35,36]. During absorption, the short

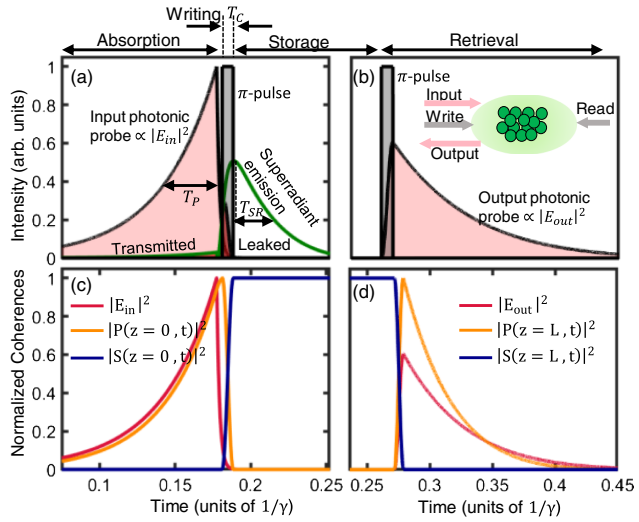

FIG. 1. SR memory protocol. (a) A short input probe (pink) with duration $T_P \ll 1/\gamma$ is absorbed by an ensemble with $d \gg 1$, and, absent the memory control, superradiantly reemits (green) with decay time $T_{\mathrm{SR}} \ll 1/\Gamma$. When a π control (gray) with a duration $T_C \ll T_{\mathrm{SR}}$ is applied, it suppresses superradiant emission and induces photonic storage. (b) Reapplying the π-pulse (gray) results in emission of the stored probe. (c) Time evolution of (normalized) photonic (pink), polarization (orange), and spin-wave (blue) coherences at the input face of the medium, showing probe storage. (d) Coherences upon readout, in backward recall. Simulation parameters $[T_P, d, T_C, B, \Omega_C, \eta]$ are $[0.037/\gamma, 50, 0.0074/\gamma, 13.3\Gamma/2\pi, 207\Gamma, 0.79]$.

incident probe builds up polarization coherence $|P(z,t)|^2$ [Fig. 1(c)] across the entire ensemble [34] on a timescale much shorter than the excited-state decoherence, which can therefore be neglected ($e^{-\gamma T_P} \approx 1$). Atomic polarization is maximized at the conclusion of the input pulse, leading to a subsequent superradiant re-emission [Fig. 1(a)]. Regardless of the line broadening mechanism (homogeneous or inhomogeneous), such re-emission occurs naturally whenever a broadband pulse is absorbed by a spectral feature with a linewidth narrower than the bandwidth of the incident pulse [21]. This absorption regime differs from that of photon-echo and FID processes, where the probe bandwidths must be smaller than or comparable to the width of the inhomogeneously broadened emitters [37].

In the writing stage, storage is achieved by converting the built-up polarization into a collective spin excitation via a control field [Fig. 1(a)] before superradiant emission proceeds. For efficient $\hat{P} \to \hat{S}$ mapping, (i) the control duration (T_C) must be much shorter than the superradiant decay time ($T_C \ll T_{\mathrm{SR}}$) ensuring minimum leakage, and (ii) the control pulse area must be π, ensuring maximum transfer [21,27,34,38]. Like all spin-wave memories, the initial coherence remains stored up to a time limited by the spin-wave decoherence. Finally, retrieval is implemented by reapplying the π pulse to map the coherence from $\hat{S} \to \hat{P} \to \hat{E}$, recovering the probe into the output photonic mode [Figs. 1(b) and 1(d)]. Bidirectional emission, as observed in some superradiance experiments [39–41], is not a factor in this memory system. The phase pattern of excited dipoles is imposed by the interference between probe and control fields, and phase matching conditions ensure that the retrieved probe is emitted into the desired mode.

To experimentally demonstrate the SR memory, we use an ensemble of $N_A \approx 2 \times 10^8$ laser-cooled ^{87}Rb atoms. With $1/e^2$ Gaussian diameters of 2.5, 3.6, and 4 mm, the cloud has volume density 7×10^9 cm^{-3} and peak optical depth $d = 9$ (along the longest direction). We form the Λ configuration on the "$D2$" line, with levels $|g\rangle \equiv |5S_{1/2}, F = 1\rangle$, $|s\rangle \equiv |5S_{1/2}, F = 2\rangle$, and $|e\rangle \equiv |5P_{3/2}, F' = 2\rangle$. The probe and control fields, resonant with the $|g\rangle \leftrightarrow |e\rangle$ and $|s\rangle \leftrightarrow |e\rangle$ transitions, are derived from two independent, phase-locked lasers, and temporally shaped via electro-optic (EOM) and acousto-optic (AOM) modulators, respectively [Fig. 2(a)]. Depending on the mean photon number per probe pulse ($\bar{n}_{\mathrm{in}}$), the control field is oriented either at $\theta = 5°$ (high $\bar{n}_{\mathrm{in}} \sim 10^3$) or $\theta = 50°$ (single-photon-level probe with $\bar{n}_{\mathrm{in}} < 1$, where the large angle permits spatial filtering of scattered control noise [42]) relative to the probe axis. The output probe is detected along the forward direction using a single-photon detector (SPD) and a time-to-digital (TDC) counter. An experimental sequence begins with ensemble preparation, followed by 1000 measurement-and-detection events performed over 1 ms.

To begin, we characterize the superradiant behavior of our cold Rb ensemble by sending short ($T_P = 20\,\mathrm{ns} < 1/\gamma = 54\,\mathrm{ns}$) probe pulses with increasing-exponential profiles and sharp switch-off [Fig. 2(b)]. The probe is almost completely absorbed up to the switch-off time, and subsequently re-emitted along the forward direction, as superradiance with characteristic time $T_{\mathrm{SR}} = 8$ ns. The observed superradiant decay time is shorter than both the input duration and the spontaneous emission lifetime [5,9,10,43–45], by factors of 2.5 and 3.5, respectively. A linewidth (Γ) measurement of the probe transition confirms no inhomogeneous broadening [46,47], which together with the probe bandwidth $2\pi B > \Gamma$, shows the conditions for superradiance are satisfied [Fig. 2(b), inset].

Next, we verify the superradiant nature of re-emission by measuring its decay time as a function of optical depth [Fig. 2(c)]. We control the optical depth between $d = 1.5$ to 9 by varying the atomic cloud's time-of-flight spatial expansion before measurement. For each d, we extract the $1/e$ decay time (T_{SR}), shown in Fig. 2(c) inset, with times from $T_{\mathrm{SR}} = (8.0 \pm 0.1)$ ns to $T_{\mathrm{SR}} = (18.8 \pm 0.8)$ ns, confirming emission's superradiant behavior: the enhancement of the decay rate with respect to optical depth is the characteristic signature of superradiance [5,9,10,43–45]. This inset also shows SR emission efficiency: the higher the d, the greater the energy contained within the emitted signal and the shorter the emission timescale, suggesting that

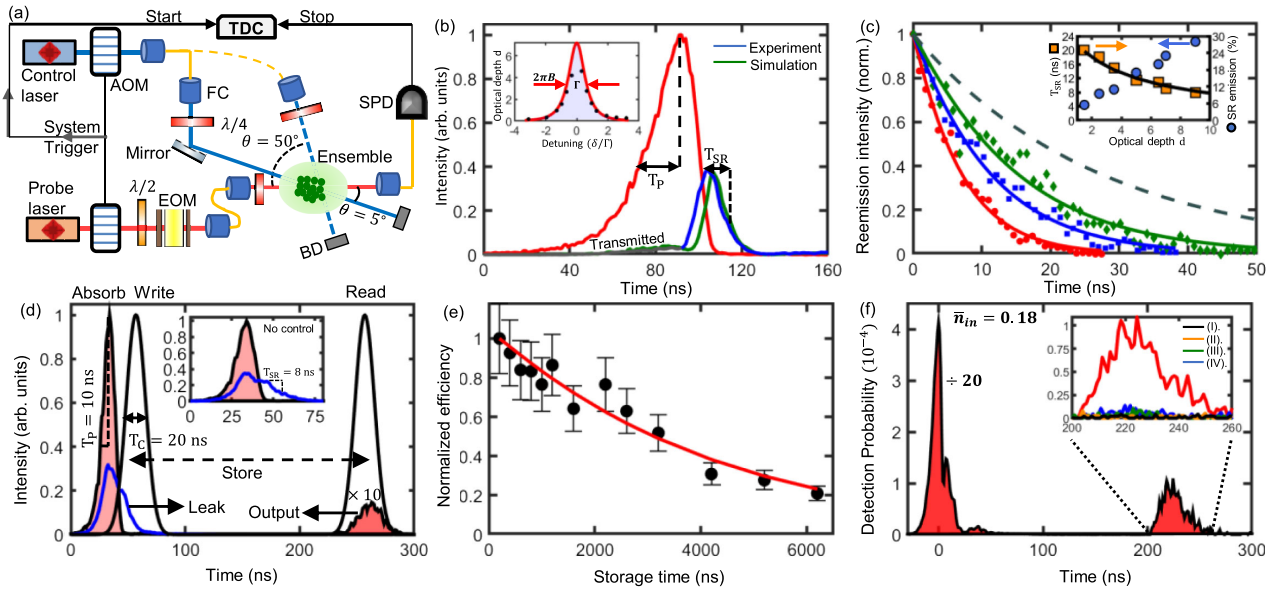

FIG. 2. Demonstration of SR memory in cold ^{87}Rb atoms. (a) Schematic of the setup. FC: fiber coupler, AOM: acousto-optic-modulator, EOM: electro-optic-modulator, SPD: single-photon-detector, TDC: time-to-digital converter, BD: beam dump. (b) Superradiant emission following an exponential probe. Inset: probe spectral profile (solid red) with bandwidth $B = 1.23\Gamma/2\pi$ for linewidth $\Gamma = 2\pi \times 6$ MHz (shaded blue). (c) Decay of the emission intensity (normalized to its own maximum) for optical depth 9 (red circles), 5 (blue squares), and 3.5 (green diamonds), with solid lines fit to the data. Black dashed line shows spontaneous-emission decay (independent of d). Inset: superradiant decay time T_{SR} and emission efficiency versus optical depth. Solid black line is fit of measured T_{SR} values using Eq. (1), which matches the probe duration for optimal storage via the SR protocol. (d) Storage and forward retrieval of a $T_P = 10$ ns, $B = 12.7$ MHz probe containing $\bar{n}_{\mathrm{in}} \gg 1$. Inset: SR emission without control. (e) Variation of memory efficiency with storage time [34]. (f) Storage and recall at the single-photon level with $\bar{n}_{\mathrm{in}} = 0.18$. Inset: memory-retrieved signal intensity relative to noise measured in four configurations (other colors) [34].

high memory efficiency requires both large optical depth (leading to an efficient polarization buildup) and fast writing.

We demonstrate the distinct operation of the SR spin-wave memory by storing an exponentially rising 10-ns probe (containing $\bar{n}_{\mathrm{in}} \approx 1.5 \times 10^3$ photons), and retrieving it along the forward direction, using Gaussian write and read control pulses of full-width-at-half-maximum duration $T_C = 20$ ns and peak power 8 mW [Fig. 2(d)]. The write control is applied 25 ns after the probe, ensuring the storage process is activated only by the SR memory mechanism [34]. By changing the time interval between write and read stages, we observe an exponential decay of the memory efficiency yielding a $1/e$ memory lifetime of (4.2 ± 0.3) μs [Fig. 2(e)], limited by the spin-wave decoherence induced by ambient magnetic fields. At 200 ns storage time, the efficiency is 3%, significantly lower than the maximum achievable SR memory efficiency of 31%, calculated for $d = 9$ and forward recall. Achieving this efficiency requires optimization of both probe and control fields.

An optimized probe is characterized by an exponentially rising temporal shape with a duration that matches the superradiant decay of our system, which makes it broadband, since $B \propto 1/T_P \approx 1/T_{\mathrm{SR}} > \Gamma$. In our demonstration, both the probe shape and duration [$T_P = 10$ ns $\approx T_{\mathrm{SR}} = 8$ ns] adequately fulfill these optimal conditions [34], but the efficiency is limited by nonoptimized control: even at our maximum power, the shortest π pulse we can generate exceeds T_{SR}, violating the condition $T_C \ll T_{\mathrm{SR}}$. As a result, a significant fraction of the polarization coherence $\hat{P}$ is lost via superradiant emission before it can be mapped to the spin wave $\hat{S}$. This loss could be eliminated by using a nanosecond-long control, which would require 2 orders of magnitude more intensity for the π pulse. Still, in the absence of such intensity, the fast-writing process is evident in these experiments. First, the temporal separation between probe and write control ensures the storage mechanisms from other protocols are suppressed [34]; second, when the system is prepared at a lower optical depth ($d = 6$) and consequently longer T_{SR} (11 ns), the maximum power acts over this longer T_{SR} and transfers a greater proportion of $\hat{P}$ to $\hat{S}$, increasing the memory efficiency (from 3% to 5%) [34]. This counterintuitive increase in efficiency for lower d under nonoptimal conditions is characteristic of the SR mechanism, and would not be found in alternate memory mechanisms. Additionally, we find that under similar conditions, the efficiency for longer probe pulses (lower bandwidths) decreases, indicating that SR memory operates best for shorter pulses, up to where T_P is comparable to T_{SR} [34].

Next, we investigate the compatibility of SR memory with quantum signals by operating with probe pulses at the

single-photon level. In particular, we measure noise from extraneously added photons during the memory operation and use this to predict fidelity for quantum state storage. We measure an unconditional noise probability of $(2.1 \pm 0.2) \times 10^{-4}$ [34], which corresponds to a stored-and-recalled signal-to-noise ratio (SNR) of 12.4 ± 1.2 for a 10-ns probe with $\bar{n}_{\text{in}} = 0.18$ [Fig. 2(f)]. If quantum states were encoded in these pulses, this SNR indicates a maximum quantum storage fidelity of $F = 1 - 1/\text{SNR} = 0.92 \pm 0.09$. Experimentally, memory efficiency remains constant across different values of $\bar{n}_{\text{in}}$, yielding a linear increase in SNR [34]. Importantly, SNR is limited only by noise from scattered control beams and not by any physical process linked to memory operation, suggesting that the SR protocol will reliably store quantum signals, such as those encoded in space, polarization, or time bins.

With these proof-of-concept results at hand, we consider future implementations by examining optimality conditions for the SR protocol. Independent of any memory approach, the "optimality" criterion dictates that the maximum achievable memory efficiency (η_{opt}) is universal and depends only on the medium's optical depth [27,31], and can be satisfied by implementing protocol-specific optimizations of both the probe and the control, under the backward-recall configuration.

Probe optimization in the SR protocol relies on both maximizing the polarization buildup and ensuring its proper spatial distribution [$P(z)$] in the absorption stage, which leads to an optimal spin-wave mode in the subsequent writing and readout stages. This is achieved by an input temporal profile that matches the time reversed replica of the superradiantly emitted pulse, both in shape and duration [22,26,48–50]. For a Lorentzian spectral feature as in our cold Rb system, inset of Fig. 2(b), the optimal shape of this probe is an exponentially rising envelope with its duration given by [21,38]

$$T_P^{\text{opt}} \approx \frac{1}{\Gamma}\left(\frac{1}{1+d/4}\right), \tag{1}$$

which corresponds to the system's T_{SR} emission time, as verified numerically and experimentally [solid fit in Fig. 2(c), inset]. For optical depths $d > 1$, the pulse time is shorter than spontaneous emission lifetime, and thus the probe bandwidth exceeds Γ, rendering this protocol inherently broadband.

Control optimization requires write-and-readout π pulses with durations T_C much shorter than T_{SR}. For square control pulses, numerical simulations verify that $T_C^{\text{opt}} \approx T_{\text{SR}}/10 \approx T_P^{\text{opt}}/10$ is sufficient for optimal efficiency, in turn requiring $\Omega_C \gg \gamma(1+d)$ for fast writing and retrieval [27,31]. For the Gaussian controls used in our experiments (with $d = 9$), this translates to a peak Rabi frequency $\Omega_C^{\text{opt}} = 130\gamma$, well above our experimental $\Omega_C^{\text{exp}} = 4.8\gamma$, accounting for the memory inefficiency.

Under optimized probe-and-control conditions, we investigate the optical-depth dependence of probe duration (bandwidth) in terms of the adiabaticity parameter ($T_P^{\text{opt}} d\gamma$). Using Eq. (1) and for $d \gg 1$, $T_P^{\text{opt}} d\gamma \leq 2$, which represents the "fast" operating regime opposite to that of adiabatic memories, which instead are characterized by $T_P^{\text{opt}} d\gamma \gg 1$ [27,31,33]. Clearly, SR memory falls into the class of nonadiabatic memories [37,51], which are inherently suitable for optimal storage of broadband signals ($2\pi B > \Gamma$). We note, however, that in homogeneously broadened media, the bandwidth of the SR control fields is ultimately limited by the spacing between ground levels. For example, storage of a one-nanosecond probe would require control fields with gigahertz spectral width, comparable to the ground-state hyperfine splitting of alkali atoms. Such broad control fields may off-resonantly excite atoms in $|g\rangle$, creating spurious spin waves that can add photonic noise at the memory output via four-wave mixing (FWM) [25,52–55].

Finally, we make a performance comparison (in terms of efficiency, optical depth, bandwidth, and control power) between SR and other memory approaches, including Autler-Townes splitting (ATS) [42,56–58] and electromagnetically induced transparency (EIT) [59–61], which are examples of nonadiabatic and adiabatic protocols, respectively. We base this comparison on typical adiabaticity parameters, corresponding to $T_P d\gamma = 2$ (SR); $T_P d\gamma = 14$ (ATS); and $T_P d\gamma = 60$ (EIT), for a broadband, exponential probe with $T_P \ll 1/\gamma$. For a given bandwidth (probe duration), the optical depth required for optimal SR efficiency is 7 times lower than in an ATS memory and 30 times lower than in an EIT memory [Fig. 3(a)]. Equivalently, for a given optical depth, the bandwidth that can be optimally stored using the SR protocol is higher than the corresponding bandwidth in the ATS and EIT protocols by the same factors, showing that SR protocol is the fastest among all protocols that are suitable for homogeneously broadened transitions [Fig. 3(b)]. Furthermore, Fig. 3(c) shows scaling of the optimal peak control intensity ($\propto \Omega_C^2$) as a function of probe bandwidth B, with $\Omega_{\text{ATS}} = 2\pi(2B)$; $\Omega_{\text{EIT}} = 2\pi(6.6B)$; and $\Omega_{\text{SR}} = 2\pi(31.2B)$, implying orders of magnitude larger control power is required for the SR protocol. In sum, SR memory operates optimally at substantially lower optical depths, but its demand on control power is significantly larger. A protocol's resource dependence (on d and Ω_C) plays a crucial role in determining the impact of fundamental noise processes on the storage fidelity. In particular, photonic four-wave-mixing (FWM) noise bears an exponential and quadratic scaling to the optical depth and control power, respectively [54,62,63], and as such, the FWM strength associated with an optimal SR memory can be a factor of 3–7 times lower than that for an adiabatic memory [34,42].

In conclusion, we experimentally demonstrated a broadband spin-wave memory based on the superradiance effect

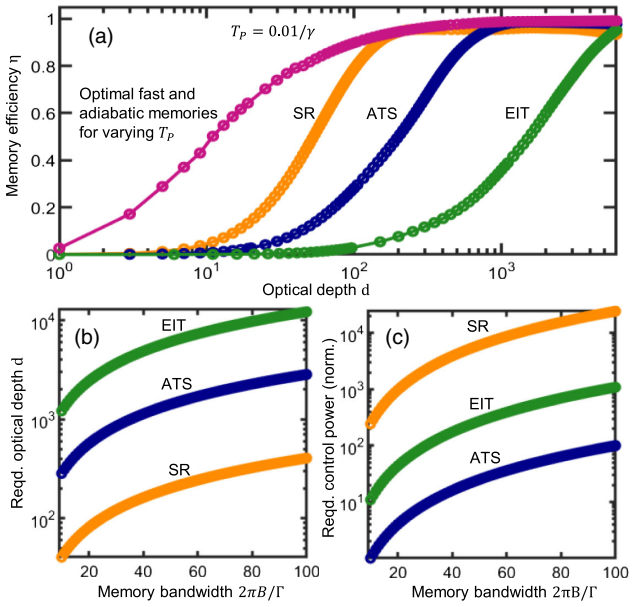

FIG. 3. Theoretical analysis of SR memory versus ATS and EIT memories for storage of broadband pulses with optimized parameters $[d, T_P, B, \Omega_C(t)]$ in backward recall. ATS and EIT protocols are optimized using [56,57]. (a) Numerically calculated memory efficiency vs optical depth for an exponential probe with $T_P = 0.01/\gamma$ ($B = 49.4\Gamma/2\pi$), showing optimal operation at ($d = 200$, $\eta = 0.93$); ($d = 1400$, $\eta = 0.96$); and ($d = 6000$, $\eta = 0.93$) for the SR, ATS, and EIT protocols, respectively. Universal optimal efficiency η_{opt} is obtained via optimal implementation of any protocol. (b) and (c) Optical depth and control power requirements versus memory bandwidth, where near-optimal operation is maintained ($\eta \geq 0.9$). Control strength is normalized with respect to the ATS power required for $B = 10\Gamma/2\pi$.

in a cold Rb gas. This memory approach offers the shortest pulse storage in systems with transition linewidths narrower than the signal bandwidth. Besides conventional platforms like atomic gases and solid state systems, a high-performance SR memory could be implemented using Bose-Einstein condensates in the originally conceived superradiant regime with large density and dimensions comparable to the excitation wavelength [1], and other interesting effects may emerge by considering subwavelength structured arrays when applied to memory [64,65]. Beyond broadband quantum memories, our results may find use in the realizations of fast and efficient heralded single photon sources [38], atom-based optical processing [66], and superradiance-mediated dipole blockade effects [67,68].

This work was supported by the University of Alberta; the Natural Sciences and Engineering Research Council, Canada (Grants No. RGPIN-04523-16, No. RGPIN-2014-06618, and No. CREATE-495446-17); the Alberta Quantum Major Innovation Fund; Alberta Innovates; and the Canada Research Chairs (CRC) Program.

*Corresponding author.
rastogi1@ualberta.ca
†Corresponding author.
lindsay.leblanc@ualberta.ca

[1] R. H. Dicke, Phys. Rev. **93**, 99 (1954).
[2] A. V. Andreev, V. I. Emel'yanov, and Y. A. Il'inski, Sov. Phys. Usp. **23**, 493 (1980).
[3] M. Gross and S. Haroche, Phys. Rep. **93**, 301 (1982).
[4] K. Cong, Q. Zhang, Y. Wang, G. T. Noe, A. Belyanin, and J. Kono, J. Opt. Soc. Am. B **33**, C80 (2016).
[5] H. S. Han, A. Lee, K. Sinha, F. K. Fatemi, and S. L. Rolston, Phys. Rev. Lett. **127**, 073604 (2021).
[6] M. O. Scully, Phys. Rev. Lett. **102**, 143601 (2009).
[7] A. A. Svidzinsky and M. O. Scully, Opt. Commun. **282**, 2894 (2009).
[8] M. O. Scully and A. A. Svidzinsky, Science **325**, 1510 (2009).
[9] M. O. Araújo, I. Krešić, R. Kaiser, and W. Guerin, Phys. Rev. Lett. **117**, 073002 (2016).
[10] S. J. Roof, K. J. Kemp, M. D. Havey, and I. M. Sokolov, Phys. Rev. Lett. **117**, 073003 (2016).
[11] C. C. Kwong, T. Yang, M. S. Pramod, K. Pandey, D. Delande, R. Pierrat, and D. Wilkowski, Phys. Rev. Lett. **113**, 223601 (2014).
[12] C. C. Kwong, T. Yang, D. Delande, R. Pierrat, and D. Wilkowski, Phys. Rev. Lett. **115**, 223601 (2015).
[13] R. Pierrat, M. Chalony, D. Delande, and D. Wilkowski, Front. Opt. 2012/Laser Sci. XXVIII **84**, LTu1I.3 (2012).
[14] N. Dudovich, D. Oron, and Y. Silberberg, Phys. Rev. Lett. **88**, 123004 (2002).
[15] L. S. Costanzo, A. S. Coelho, D. Pellegrino, M. S. Mendes, L. Acioli, K. N. Cassemiro, D. Felinto, A. Zavatta, and M. Bellini, Phys. Rev. Lett. **116**, 023602 (2016).
[16] M. O. Scully, E. S. Fry, C. H. Ooi, and K. Wódkiewicz, Phys. Rev. Lett. **96**, 010501 (2006).
[17] A. A. Svidzinsky, J. T. Chang, and M. O. Scully, Phys. Rev. Lett. **100**, 160504 (2008).
[18] T. Bienaimé, M. Petruzzo, D. Bigerni, N. Piovella, and R. Kaiser, J. Mod. Opt. **58**, 1942 (2011).
[19] R. T. Sutherland and F. Robicheaux, Phys. Rev. A **93**, 023407 (2016).
[20] S. L. Bromley, B. Zhu, M. Bishof, X. Zhang, T. Bothwell, J. Schachenmayer, T. L. Nicholson, R. Kaiser, S. F. Yelin, M. D. Lukin, A. M. Rey, and J. Ye, Nat. Commun. **7**, 11039 (2016).
[21] V. C. Vivoli, N. Sangouard, M. Afzelius, and N. Gisin, New J. Phys. **15**, 095012 (2013).
[22] A. Walther, A. Amari, S. Kröll, and A. Kalachev, Phys. Rev. A **80**, 012317 (2009).
[23] A. I. Lvovsky, B. C. Sanders, and W. Tittel, Nat. Photonics **3**, 706 (2009).
[24] K. Hammerer, J. Sherson, B. Julsgaard, J. I. Cirac, and E. S. Polzik, Quantum Inf. with Contin. Var. Atoms Light **82**, 513 (2007).
[25] K. Heshami, D. G. England, P. C. Humphreys, P. J. Bustard, V. M. Acosta, J. Nunn, and B. J. Sussman, J. Mod. Opt. **63**, 2005 (2016).
[26] A. Kalachev, Phys. Rev. A **76**, 043812 (2007).
[27] A. V. Gorshkov, A. André, M. D. Lukin, and A. S. Sørensen, Phys. Rev. A **76**, 033805 (2007).

[28] The term "superradiance" may refer both to the case of externally imposed dipoles (as in this Letter) and the case of what is also commonly referred to as "superfluorescence," in which dipoles self-align after a spontaneous emission event. The emission properties in both cases are the same.
[29] N. Sangouard, C. Simon, H. de Riedmatten, and N. Gisin, Rev. Mod. Phys. **83**, 33 (2011).
[30] H. J. Kimble, Nature (London) **453**, 1023 (2008).
[31] A. V. Gorshkov, A. André, M. Fleischhauer, A. S. Sørensen, and M. D. Lukin, Phys. Rev. Lett. **98**, 123601 (2007).
[32] N. Sangouard, C. Simon, M. Afzelius, and N. Gisin, Phys. Rev. A **75**, 032327 (2007).
[33] J. Nunn, I. A. Walmsley, M. G. Raymer, K. Surmacz, F. C. Waldermann, Z. Wang, and D. Jaksch, Phys. Rev. A **75**, 011401(R) (2007).
[34] See Supplemental Material at http://link.aps.org/supplemental/10.1103/PhysRevLett.129.120502 for more information.
[35] R. Finkelstein, E. Poem, O. Michel, O. Lahad, and O. Firstenberg, Sci. Adv. **4**, eaap8598 (2018).
[36] K. T. Kaczmarek, P. M. Ledingham, B. Brecht, S. E. Thomas, G. S. Thekkadath, O. Lazo-Arjona, J. H. D. Munns, E. Poem, A. Feizpour, D. J. Saunders, J. Nunn, and I. A. Walmsley, Phys. Rev. A **97**, 042316 (2018).
[37] W. Tittel, M. Afzelius, T. Chanelière, R. L. Cone, S. Kröll, S. A. Moiseev, and M. Sellars, Laser Photonics Rev. **4**, 244 (2010).
[38] M. Ho, C. Teo, H. D. Riedmatten, and N. Sangouard, New J. Phys. **20**, 123018 (2018).
[39] L. E. Sadler, J. M. Higbie, S. R. Leslie, M. Vengalattore, and D. M. Stamper-Kurn, Phys. Rev. Lett. **98**, 110401 (2007).
[40] A. Hilliard, F. Kaminski, R. le Targat, C. Olausson, E. S. Polzik, and J. H. Müller, Phys. Rev. A **78**, 051403(R) (2008).
[41] H. Uys and P. Meystre, Phys. Rev. A **75**, 033805 (2007).
[42] E. Saglamyurek, T. Hrushevskyi, A. Rastogi, L. W. Cooke, B. D. Smith, and L. J. LeBlanc, New J. Phys. **23**, 043028 (2021).
[43] S. Zhang, C. Liu, S. Zhou, C.-S. Chuu, M. M. T. Loy, and S. Du, Phys. Rev. Lett. **109**, 263601 (2012).
[44] S. Jennewein, M. Besbes, N. J. Schilder, S. D. Jenkins, C. Sauvan, J. Ruostekoski, J.-J. Greffet, Y. R. P. Sortais, and A. Browaeys, Phys. Rev. Lett. **116**, 233601 (2016).
[45] S. Jennewein, L. Brossard, Y. R. P. Sortais, A. Browaeys, P. Cheinet, J. Robert, and P. Pillet, Phys. Rev. A **97**, 053816 (2018).
[46] J. J. Maki, M. S. Malcuit, M. G. Raymer, R. W. Boyd, and P. D. Drummond, Phys. Rev. A **40**, 5135 (1989).
[47] M. S. Malcuit, J. J. Maki, D. J. Simkin, and R. W. Boyd, Phys. Rev. Lett. **59**, 1189 (1987).
[48] A. Walther, A. Amari, S. Kröll, and A. Kalachev, Phys. Rev. A **80**, 012317 (2009).
[49] M. Stobińska, G. Alber, and G. Leuchs, Europhys. Lett. **86**, 14007 (2009).
[50] H. L. Dao, S. A. Aljunid, G. Maslennikov, and C. Kurtsiefer, Rev. Sci. Instrum. **83**, 083104 (2012).
[51] A. V. Gorshkov, A. André, M. D. Lukin, and A. S. Sørensen, Phys. Rev. A **76**, 033806 (2007).
[52] N. B. Phillips, A. V. Gorshkov, and I. Novikova, Phys. Rev. A **83**, 063823 (2011).
[53] P. S. Michelberger, T. F. M. Champion, M. R. Sprague, K. T. Kaczmarek, M. Barbieri, X. M. Jin, D. G. England, W. S. Kolthammer, D. J. Saunders, J. Nunn, and I. A. Walmsley, New J. Phys. **17**, 043006 (2015).
[54] N. Lauk, C. O'Brien, and M. Fleischhauer, Phys. Rev. A **88**, 013823 (2013).
[55] S. E. Thomas, T. M. Hird, J. H. D. Munns, B. Brecht, D. J. Saunders, J. Nunn, I. A. Walmsley, and P. M. Ledingham, Phys. Rev. A **100**, 033801 (2019).
[56] E. Saglamyurek, T. Hrushevskyi, A. Rastogi, K. Heshami, and L. J. LeBlanc, Nat. Photonics **12**, 774 (2018).
[57] A. Rastogi, E. Saglamyurek, T. Hrushevskyi, S. Hubele, and L. J. Leblanc, Phys. Rev. A **100**, 012314 (2019).
[58] E. Saglamyurek, T. Hrushevskyi, L. Cooke, A. Rastogi, and L. J. LeBlanc, Phys. Rev. Research **1**, 022004(R) (2019).
[59] M. Fleischhauer and M. D. Lukin, Phys. Rev. Lett. **84**, 5094 (2000).
[60] M. Fleischhauer and M. D. Lukin, Phys. Rev. A **65**, 022314 (2002).
[61] Y. F. Hsiao, P. J. Tsai, H. S. Chen, S. X. Lin, C. C. Hung, C. H. Lee, Y. H. Chen, Y. F. Chen, I. A. Yu, and Y. C. Chen, Phys. Rev. Lett. **120**, 183602 (2018).
[62] G. Romanov, C. O'Brien, and I. Novikova, J. Mod. Opt. **63**, 2048 (2016).
[63] J. Geng, G. T. Campbell, J. Bernu, D. B. Higginbottom, B. M. Sparkes, S. M. Assad, W. P. Zhang, N. P. Robins, P. K. Lam, and B. C. Buchler, New J. Phys. **16**, 113053 (2014).
[64] A. Asenjo-Garcia, M. Moreno-Cardoner, A. Albrecht, H. J. Kimble, and D. E. Chang, Phys. Rev. X **7**, 031024 (2017).
[65] K. E. Ballantine and J. Ruostekoski, Phys. Rev. Research **2**, 023086 (2020).
[66] M. Mazelanik, M. Parniak, A. Leszczyński, M. Lipka, and W. Wasilewski, npj Quantum Inf. **5**, 22 (2019).
[67] A. Cidrim, T. S. do Espirito Santo, J. Schachenmayer, R. Kaiser, and R. Bachelard, Phys. Rev. Lett. **125**, 073601 (2020).
[68] L. A. Williamson, M. O. Borgh, and J. Ruostekoski, Phys. Rev. Lett. **125**, 073602 (2020).